CASSCF/CAS-PT2 Study of Hole Transfer in Stacked DNA Nucleobases

Lluís Blancafort*,† and Alexander A. Voityuk*,†,‡

Institut de Química Computational, Departament de Química, Universitat de Girona, 17071 Girona, Spain, and Institució Catalana de Recerca i Estudis Avançats, Barcelona 08010, Spain

Received: February 24, 2006; In Final Form: April 2, 2006

CASSCF and CAS-PT2 calculations are performed for the ground and excited states of radical cations consisting of two and three nucleobases. The generalized Mulliken−Hush approach is employed for estimating electronic couplings for hole transfer in the π-stacks. We compare the CASSCF results with data obtained within Koopmans' approximation. The calculations show that an excess charge in the ground and excited states in the systems is quite localized on a single base both at the CASSCF level and in Koopmans' picture. However, the CASSCF calculations point to a larger degree of localization and, in line with this, smaller transition dipole moments. The agreement between the CAS-PT2 corrected energy gaps and the values estimated with Koopmans' theorem is better, with the CAS-PT2 calculations giving somewhat smaller gaps. Overall, both factors result in smaller CASSCF/CAS-PT2 couplings, which are reduced by up to 40% of the couplings calculated using Koopmans' approximation. The tabulated data can be used as benchmark values for the electronic couplings of stacked nucleobases. For the base trimers, comparison of the results obtained within two- and three-state models show that the multistate treatment should be applied to derive reliable estimates. Finally, the superexchange approach to estimate the donor acceptor electronic coupling in the stacks GAG and GTG is considered.

Introduction

The last 15 years have been very important for understanding mechanisms of charge transfer (CT) through DNA π-stacks.[1] The majority of experimental[2−6] and theoretical studies[7−18] of charge transfer in DNA have been related to radical-cation states. Because guanine (G) is the most easily oxidized nucleobase, the cation radical G^+ is a key intermediate in the hole transfer process mediated by DNA. Created initially adjacent to an oxidant, the charge hops through the stack using guanine bases as stepping stones. As a result, G^+ can be generated in DNA far away from the oxidant because of the hole transfer process. When donor and acceptor (GC) pairs are separated by a short $(AT)_n$ bridge ($n \leq 3$), each elementary hopping step $G_i^+ \rightarrow G_j$ can be represented as superexchange tunneling. The superexchange mechanism is characterized by a fast exponential decay of the HT rate with the donor−acceptor distance R and is operative at short distances, $R \leq 15$ Å. Although in principle single-step tunneling allows for long-range charge transfer, its efficiency becomes very low. Multistep hole hopping gives rise to long-range charge transport ($R \leq 200$ Å). The mechanism may be described as G-hopping, a series of tunneling steps between guanines separated by AT pairs. When guanines are separated by more than three AT pairs, hole hopping between adenine bases, A-hopping, may also become operative.[19,20] The A-hopping mechanism has been considered in several theoretical studies.[9,12,17]

An alternative mechanism, phonon-assisted polaron hopping, is considered by Conwell[21] and Schuster.[22] In this case, hole transport in DNA has been treated theoretically within the adiabatic models. These models assume that the excess positive charge is extended over several bases in the stack. However, recently, it has been demonstrated that charge delocalization in DNA is essentially suppressed by polar environment and hole states are localized on individual guanines even in sequences consisting only of GC pairs.[23] Therefore, the motion of a positive charge can be viewed as a series of hops between G sites. This result does not support the suggestion of Basko and Conwell[24] that the hole charge is spread over five or more neighboring base pairs, leading to polaron formation in DNA stacks.

In a DNA π-stack, where donor and acceptor are separated by one or more intervening base pairs, CT is expected to fall well within the nonadiabatic regime.[15] In this case, the rate of CT is proportional to the square of the electronic coupling V_{da} between the donor and acceptor sites.[25,26] Therefore, the electronic coupling plays an important role in modulating the efficiency of CT in these cases. The application of different models to estimate V_{da} in DNA stacks has been discussed recently.[27]

In most studies of charge transfer in DNA, the one-electron or Koopmans' theorem approximation (KTA) has been used to calculate the electronic coupling.[12,14,15,17,27] Within this scheme, the properties of adiabatic states for a radical cation can be approximated using one-electron energies and occupied MO of the corresponding neutral (close-shell) system (some details are provided in the next section). While KTA appears to be physically reasonable for estimating electronic couplings, more sophisticated calculations are needed to assess the accuracy of this approach.

The purpose of the paper is to study the electron-correlation effects on the coupling in DNA π-stacks and to calculate the matrix elements beyond the one-electron approximation, to establish better benchmarks than those based on KTA. In particular, the couplings are calculated here from the energy

* To whom correspondence should be addressed. E-mail: lluisb@stark.udg.es; alexander.voityuk@icrea.es.
† Universitat de Girona.
‡ Institució Catalana de Recera i Estudis Avançats.

10.1021/jp061184s CCC: $33.50
Published on Web 05/02/2006

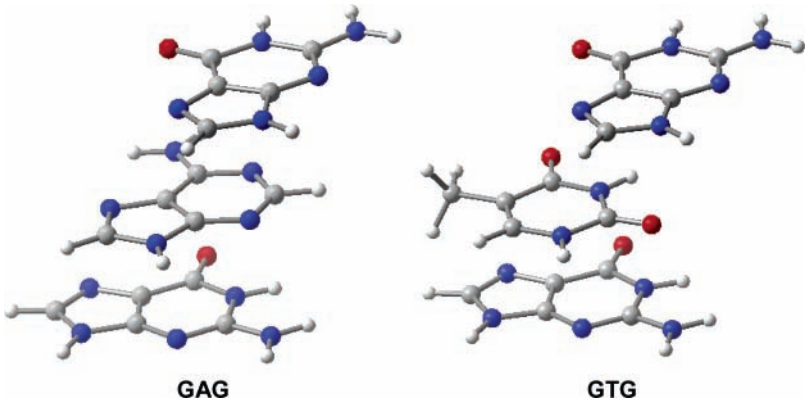

Figure 1. GAG and GTG structures.

gaps and transition dipole moments between the ground and excited electronic states of a radical cation rather than from the orbital energies and dipole moment matrix elements for the corresponding neutral system, as assumed within KTA. Thus, we have used multireferential methods (complete active space self-consistent field, CASSCF and its second-order perturbation formulation, CAS-PT2) for the calculation of electronic coupling in single-strand DNA stacks consisting of two and three nucleobases. Then, we have focused on the role of the bridge states in mediation of the donor−acceptor coupling for hole transfer between guanine bases in the radical-cations GAG and GTG (Figure 1).

The CASSCF and CAS-PT2 levels of theory should be more adequate for the present application than the calculation of the excited states with time-dependent density functional (TD-DFT) methods because of the known limitations of the latter methods with charge-transfer excitations.[28] On the other hand, the use of CASSCF for the present problem has the shortcomings that dynamic correlation is not included and that the size of the system imposes the use of "reduced" active spaces with respect to the desirable ones. CAS-PT2 calculations (including the multistate formulation, MS-PT2) have been carried out to overcome these disadvantages. Overall, the results show that the couplings recalculated at this level of theory are reduced by up to 40% with respect to the KTA-based values, due to higher charge localization (i.e., smaller transition dipole moments) and smaller energy gaps. KTA, however, provides relatively good estimations for the ground- to excited-state energy gaps in the present systems. According to test calculations that we have performed for some examples, these estimations are better than the excitation energies obtained with configuration interaction with singles (CIS) and TD-DFT.

Computational Details

CASSCF Calculations. The Hartree−Fock and CASSCF calculations are carried out for several one-strand DNA stacks consisting of two and three nucleobases using the standard 6-31G* basis set. The program Gaussian03 was employed.[29] For the radical cations of the stacked dimers, the energies of the ground and excited states are obtained from a single calculation, using state-averaged orbitals with equal weights for each state. The dipole moments of each state and the transition dipole moments between the two states are derived from the same calculation. A similar strategy is followed for the trimer calculations, considering three instead of two states and calculating all transition dipole moments between the three states. For a better estimation of the dimer energies, these are recalculated with the program MOLCAS 5.4[30] at the CAS-PT2 level, with a level shift parameter of 0.2. The multistate formulation of CAS-PT2, MS-PT2, which accounts for the nonorthogonality of the CAS-PT2 wave functions, is used for a further refinement of the energy gaps. However, the changes with respect to the CAS-PT2 energy gaps are negligible except for the AA case (see Results and Discussion section). The transition dipole moments are not recalculated at the CAS-PT2 level, and the CAS-PT2 energies of the trimers were not calculated because of computational limitations.

The key aspect of the CASSCF calculations performed here is the selection of the active space. For the three bases, it is possible to define a "full" (or "ideal") set of active space orbitals formed by the π-orbitals (the in-plane, oxygen, or nitrogen lone pairs were not considered here because they lie perpendicular to the stacking axis of the molecule). This gives "full" active spaces of 11, 10, and 8 π-orbitals for guanine, adenine, and thymine, respectively, that is, 19 to 22 orbitals for the dimers considered here. These active spaces had to be reduced to 11 electrons in 12 orbitals to keep the calculations feasible, with 6 orbitals coming from each base to ensure a balanced treatment of the two states. To increase the active space in a balanced way, 2 more orbitals for each base are necessary, which would result in 16 orbitals and an approximately 200-fold increase in the number of spin-adapted configuration state functions. Thus, the active space of 12 orbitals is a limit for the CASSCF calculations with our present resources. For the base trimers, the same active space of 11 electrons in 12 orbitals was used, that is, the number of orbitals on each base was reduced to 4. This is equivalent to a CAS(7,8) active space for the dimers. Therefore, the calculations for the dimers were repeated with the CAS(7,8) active space, and the results are compared below.

Estimation of Electronic Couplings. The generalized Mulliken−Hush (GMH) method introduced by Cave and Newton was employed to calculate electronic couplings.[31,32] In dimer systems, we consider only two adiabatic states (the ground and first excited states). Within the two-state model, the electronic coupling can be expressed via the vertical excitation energy $E_2 - E_1$, the difference $\mu_1 - \mu_2$ of the adiabatic dipole moments, and the transition dipole moment μ_{12}

$$V_{da} = \frac{(E_2 - E_1)|\mu_{12}|}{\sqrt{(\mu_1 - \mu_2)^2 + 4\mu_{12}^2}} = \frac{(E_2 - E_1)|\mu_{12}|}{|\mu_d - \mu_a|} \qquad (1)$$

The difference of the diabatic dipole moments of donor and acceptor $|\mu_d - \mu_a|$ can be expressed as $((\mu_1 - \mu_2)^2 + 4\mu_{12}^2)^{1/2}$.[31,32] The GMH method allows the calculation of V_{da} in various systems, independent of symmetry and geometrical constraints. For the donor−bridge−acceptor complexes GAG

and GTG, both three- and two-state GMH models were applied. In these systems, the electronic levels of the bridge are energetically close to those of the donor and acceptor, and the diabatic states represent a combination of three adiabatic states. Therefore, the three-state model should be employed. A transformation of adiabatic states to diabatic states proceeds using the unitary matrix T which diagonalizes the adiabatic dipole moment matrix

$$V_{da} = \sum T_{id} E_i T_{ia} \tag{2}$$

where E is the diagonal matrix of the adiabatic energies. Expressions 1 and 2 can be applied to adiabatic states found within different quantum chemical approaches. In many cases, one can reliably calculate electron-transfer matrix elements on the basis of the one-electron approximation.

It is worth noting that within GMH one uses projections of the transition and dipole moments onto a predetermined axis rather than the length of these vectors. The axis can coincide with the direction of the difference of adiabatic ($\mu_2 - \mu_1$) or diabatic ($\mu_a - \mu_d$) dipole moments or with the direction of the transition moment μ_{12}. In a π-stack, it is convenient to employ the components along the direction which is perpendicular to the planes of the donor and acceptor. The resulting couplings remain almost unchanged when different (but physically reasonable) axes are used to define the projections of the dipole and transition moments.

Koopmans' Theorem Approximation (KTA). As an example, let us discuss hole transfer in a stack GTG. The radical-cation states G^+TG and GTG^+ represent the initial and final states of the CT reaction between the guanine bases. Within CASSCF, the adiabatic splitting $\Delta = E_2 - E_1$ of the electronic states is calculated as the first excitation energy of the radical cation. Alternatively, invoking KTA, Δ can be estimated as the difference of the one-electron energies of the two highest occupied molecular orbitals HOMO and HOMO-1 calculated for the closed-shell neutral system GTG. Within this approximation, distribution of the excess charge in the ground state of the radical cation can be estimated via the corresponding Mulliken populations of the HOMO of the neutral system. Then, the charge on a fragment F can be estimated as

$$q_1(F) = \sum_{i \in F} C_{i,\mathrm{HOMO}} \sum_{j=1}^{N} C_{j,\mathrm{HOMO}} S_{ij} \tag{3}$$

Here, S_{ij} is the overlap of atomic orbitals (AOs) i and j; i runs over atomic orbitals associated with the fragment F while j runs over all AOs. The fragment charges in the first excited state are calculated similarly using the coefficients HOMO-1. Then, the relative energy of the bridge state can be estimated as a difference of the orbital energies of HOMO-2 and HOMO.

To apply the GMH method, eqs 1 and 2, one has to estimate the difference of the adiabatic dipole moments ($\mu_1 - \mu_2$) and the transition moment μ_{12} within KTA

$$\mu_1 - \mu_2 = \sum_{i,j=1}^{M} (C_{i,\mathrm{HOMO}} C_{j,\mathrm{HOMO}} - C_{i,\mathrm{HOMO-1}} C_{j,\mathrm{HOMO-1}}) d_{ij} \tag{4}$$

$$\mu_{12} = -\sum_{i,j=1}^{M} C_{i,\mathrm{HOMO}} C_{j,\mathrm{HOMO-1}} d_{ij} \tag{5}$$

Here, d_{ij} are the matrix elements of the dipole operator defined for AOs i and j.

TABLE 1: Mulliken Charges on Nucleobases in Dimers

		ground state		excited state	
5-XY-3	method	Q(X)	Q(Y)	Q(X)	Q(Y)
GG	KTA	0.965	0.035	0.040	0.960
	CAS(7,8)	0.965	0.035	0.033	0.967
	CAS(11,12)	0.976	0.024	0.025	0.975
AA	KTA	0.186	0.814	0.816	0.186
	CAS(7,8)	0.304	0.696	0.688	0.312
	CAS(11,12)	0.010	0.990	0.987	0.013
AG	KTA	0.078	0.922	0.923	0.077
	CAS(7,8)	0.011	0.989	0.988	0.012
	CAS(11,12)	0.024	0.976	0.975	0.025
GA	KTA	0.971	0.029	0.036	0.964
	CAS(7,8)	0.990	0.010	0.015	0.985
	CAS(11,12)	0.992	0.008	0.015	0.985
TG	KTA	0.008	0.992	.993	0.007
	CAS(7,8)	0.006	0.994	0.992	0.008
	CAS(11,12)	0.008	0.992	0.990	0.010
GT	KTA	0.988	0.012	0.019	0.981
	CAS(7,8)	0.996	0.004	0.017	0.983
	CAS(11,12)	0.992	0.008	0.026	0.974
G_G	KTA	>0.999	<0.001	<0.001	>0.999
	CAS(7,8)	>0.999	<0.001	<0.001	>0.999
	CAS(11,12)	>0.999	<0.001	<0.001	>0.999

Geometries. Experimental idealized atomic coordinates of the three bases (adenine, guanine, and thymine) taken from high-resolution X-ray and neutron studies were used for generating the structures.[33] The mutual positions of the nucleobases in the models studied correspond to a regular B-DNA structure. The geometries of the systems were constructed with the program SCHNArP. [34]

Results and Discussion

Localization of Hole Charge. As noted in the Introduction, the mechanism of the charge transfer strongly depends on whether the hole is localized or spread over several nucleobases. In Table 1, we compare the charge distribution in the dimers derived from CASSCF calculations with KTA-based estimates. The CASSCF values calculated with the (7,8) and (11,12) are reported in Table 1 to show that there is a good agreement between both methods, but we focus our discussion on the CASSCF(11,12) values. In general, the excess charge is quite localized on individual nucleobases in both the ground and excited states. For example, in the GG dimer, the excess charge is almost completely confined to the first base (5′-G) in the ground state and to the second base (G-3′) in the excited state. Earlier it was shown that the 5′-G in GG and both G on the 5′-side in GGG have the lowest oxidation potential in line with experimental findings.[35,36] The effects of solvation and internal reorganization on the hole charge distribution in sequences 5′-X-GG-Y-3′ have been considered recently.[37] However, distinct from GG, the excess charge in the AA dimer is localized on the second base (A-3′) in the ground state. The difference is mainly due to the electrostatic interaction of the fragments.

As seen from Table 1, there is a good qualitative agreement in the charge distributions between the fragments calculated with the CASSCF and KTA methods, except for the AA case. This justifies the conclusions obtained within the KTA scheme that the excess charge in DNA π-stacks should be quite localized.[13−17] However, the quantitative differences between the KTA and CASSCF(11,12) charge distributions result in significant differences (up to a factor of 2) in the transition dipole moments, as the charge distribution in the fragments and the magnitude of the transition dipole moments are closely related.[38] This effect is particularly clear for the AG and GA cases, and it leads to smaller electronic couplings at the CASSCF level.

TABLE 2: Mulliken Charges on Nucleobases in the GAG and GTG Systems

	ground state			excited state 1			excited state 2		
5-G_1BG_3-3	$Q(G_1)$	Q(B)	$Q(G_3)$	$Q(G_1)$	Q(B)	$Q(G_3)$	$Q(G_1)$	Q(B)	$Q(G_3)$
GAG KTA	0.904	0.088	0.008	0.026	0.055	0.919	0.076	0.852	0.072
CAS(11,12)	0.951	0.037	0.012	0.018	0.042	0.940	0.037	0.907	0.057
GTG KTA	0.982	0.017	0.001	0.002	0.008	0.990	0.021	0.971	0.008
CAS (11,12)	0.991	0.006	0.003	0.006	0.000	0.994	0.016	0.974	0.010

TABLE 3: Excitation Energy (ΔE_{12}), Transition Dipole Moment (μ_{12}^z), and Electronic Coupling V in Nucleobase Dimers Calculated with KTA, CASSCF, and CAS-PT2

5-XY-3	method	ΔE_{12}, eV	μ_{12}^z,au	V, eV	ΔE_{12}(KTA)/ ΔE_{12}(PT2)	μ_{12}^z(KTA)/ μ_{12}^z(CAS)
GG	KTA	0.472	1.120	0.083	120%	137%
	CAS(7,8)	0.414	1.015	0.067		
	CAS(11,12)	0.370	0.819	0.049		
	CAS-PT2(11,12)	0.392		0.051		
GA	KTA	0.551	1.022	0.089	98%	249%
	CAS(7,8)	0.892	0.374	0.054		
	CAS(11,12)	0.713	0.410	0.046		
	CAS-PT2(11,12)	0.560		0.036		
AG	KTA	0.185	1.667	0.049	54%	204%
	CAS(7,8)	0.593	0.475	0.045		
	CAS(11,12)	0.463	0.817	0.061		
	CAS-PT2(11,12)	0.340		0.044		
GT	KTA	1.574	0.548	0.137	134%	129%
	CAS(7,8)	1.799	0.340	0.098		
	CAS(11,12)	1.415	0.424	0.097		
	CAS-PT2(11,12)	1.175		0.081		
TG	KTA	1.153	0.476	0.085	145%	98%
	CAS(7,8)	1.235	0.445	0.087		
	CAS(11,12)	1.097	0.484	0.084		
	CAS-PT2(11,12)	0.797		0.061		
AA	KTA	0.078	2.456	0.030	80%	10%
	CAS(7,8)	0.144	2.810	0.066		
	CAS(11,12)	0.047	0.256	0.002		
	CAS-PT2(11,12)	0.097		0.004		
G_G	KTA	0.189	0.0014	$0.021\ 10^{-3}$	113%	22%
	CAS(7,8)	0.171	0.0057	$0.076\ 10^{-3}$		
	CAS(11,12)	0.166	0.0074	$0.095\ 10^{-3}$		
	CAS-PT2(11,12)	0.167		$0.096\ 10^{-3}$		

The analysis of the fragment charges also reveals a difficulty with the calculation of the couplings for the AA case. Thus, the charge delocalization at the KTA, CASSCF(7,8), and CASSCF(11,12) levels of theory ranges from 30% to 1%. This results in large differences in the calculated couplings (see Table 3) of more than an order of magnitude. The CAS(11,12) predicts almost complete charge localization on the fragments and a very small coupling ($V_{ab} < 0.01$ eV). However, in view of the difference between the CASSCF(7,8) and CASSCF(11,12) values for this particular case, a calculation with a larger active space (16 orbitals or more) would be desirable to confirm the latter result. This is not possible at present, and therefore, the AA results will not be considered further. However, we note that the AG and GA show a much smaller dependence on the CASSCF active space, and therefore, the results for GAG should be significant.

Turning to the GAG and GTG trimers (Table 2), the ground-state hole charge is mainly localized on the first nucleobase 5'-G (hole donor). In GAG, a remarkable portion of the charge is also found on the bridge (0.09 and 0.04 according to the KTA and CASSCF calculations, respectively). By the lowest excitation, the charge is transferred to the hole acceptor G_3. Again, about 5% of the positive charge is on adenine. The delocalization of the charge over the bridge suggests that the two-state model for estimation of the diabatic properties of the hole donor and acceptor may be inaccurate in this case. This point will be discussed later in more detail. In the second excited state, the hole is mainly localized on adenine; nonnegligible positive charges are found on the donor and acceptor sites, and the CASSCF values are 0.04 and 0.06.

Effect of the Active Space. Let us briefly consider the influence of reducing the active space on the calculated charge distribution. This point is closely related to the accuracy of the dipole moment matrix elements, since these depend on the transition one-electron density matrixes, which in turn depend on the charge distribution for the states. We start with charge distribution on the single bases. We calculated the Mulliken charges on the heavy atoms in the radical cations of guanine, adenine, and thymine using different active spaces (see Supporting Information, Tables SI1a−SI1c). The reduction of the active space has only a small effect on the charge distribution, which remains qualitatively similar for different active spaces. In addition to that, comparison of Mulliken charges and dipole moments in dimers (Tables 1 and 3) also shows that the values derived from the calculation with CAS(11,12) are well reproduced with data obtained using a smaller active space, CAS(7,8), with the exception of the AA pair, as noted above. Overall, these results give us confidence on the use of the reduced active spaces (4 orbitals per base) for the calculation of the dipole and transition dipole moments of the GAG and GTG trimers.

Electronic Coupling in the Dimer Systems. In line with the two-state GMH model, eq 1, the coupling is proportional to the excitation energy and the transition dipole moment. The calculated excitation energies, transition dipole moments, and the corresponding electronic couplings, obtained using KTA, CASSCF with different sizes of the active space, and CAS-

TABLE 4: Calculated Parameters of Single-strand Stacks GTG and GAG

stack	GAG		GTG	
method	KTA	CASSCF	KTA	CASSCF
ΔE_{12}, eV	0.185	0.118	0.188	0.178
ΔE_{13}, eV	0.340	0.345	1.247	1.239
μ^z_{12},au	1.512	1.376	0.456	0.068
μ^z_{13},au	1.433	0.916	0.664	0.398
μ^z_{23},au	1.885	1.523	0.548	0.496
V_{db}, eV[a]	**0.059** 0.077	**0.036** 0.049	**0.126** 0.131	**0.078** 0.078
V_{ba}, eV[a]	**0.041** 0.044	**0.052** 0.052	**0.092** 0.089	**0.082** 0.082
V_{da}, eV[a]	**0.037** 0.024	**0.021** 0.013	**0.017** 0.007	**0.007** 0.001

[a] Electronic couplings given in bold and regular fonts were calculated using the three-state and two-state models, respectively.

PT2, are listed in Table 3. We note that the difference of diabatic dipole moments $|\mu_d - \mu_a|$ in the dimers is the same for all considered systems (approximately 6.3 au or 16 D), as it is determined by the distance between planes of the nucleobases. The CASSCF/CAS-PT2 couplings were calculated using the CASSCF(11,12) transition dipole moments and CAS-PT2 energy gaps and are referred to as CAS-PT2 values in our discussion and in Table 3.

The differences between the KTA- and CAS-PT2-based couplings are the result of the changes in the excitations energies and the transition dipole moments. In general, the CAS-PT2 and CASSCF values for the energy gaps and transition dipoles, respectively, are smaller than with KTA, and this leads to smaller CAS-PT2 couplings. The relative ordering of the couplings for the dimers also changes with the two methodologies. Besides, the agreement of the KTA couplings with the CASSCF(11,12) ones is better than with the CAS-PT2 values because the CASSCF(11,12) energy gaps are larger and closer to the KTA ones. The only exception to the trend that KTA overestimates the energy gaps with respect to CAS-PT2 is AG, where the CAS-PT2 energy gap is larger than the KTA one. This explains the good agreement between the AG electronic couplings with the two methodologies.

The transition dipole moments are up to 40% smaller at the CASSCF(11,12) level than with KTA. However, this trend is inverted for the G_G system, which was generated by removing the adenine base from GAG. Here, the transition dipoles are about 2 orders of magnitude smaller than those for the remaining dimers because of the large separation between the bases. Thus, for both methods, the delocalization of the hole charge in G_G is less than 10^{-5} au, but within CASSCF, it is found to be slightly higher and this could be the reason for the inversion in the trend.

The agreement between the CAS-PT2 and KTA-based energy gaps is better than that for the transition dipoles. In this respect, the KTA-based energy gaps in the present stacked systems appear to be more reliable than the ones obtained with CIS or TD-DFT excited-state calculations on the radical cations, as we have observed in several test calculations. KTA also reproduces the trends in directional asymmetry found with CAS-PT2 for the energy gaps in the guanine−adenine and guanine−thymine stacked pairs, where the energy gaps for GA and GT are larger than those for AG and TG, respectively, due to the different stabilizations of the hole charges in the 3′ and 5′ positions.[39] In addition to that, there is also very good agreement between the KTA-based and the CAS-PT2 energy gaps for the base trimers (see Table 4).

Electronic Coupling in GAG and GTG Stacks. Table 4 lists the excitation energies, transition moments, and electronic couplings calculated with KTA and CASSCF (the GAG and GTG stacks were calculated using an active space composed of 4 orbitals per base, that is, a total (11,12) active space, and the CAS-PT2 energy was not calculated). The energy gaps estimated with both schemes are in good agreement, while KTA overestimates the transition dipole moments. As a result, the couplings calculated for the trimers are significantly lower at the CASSCF level than based on KTA, which is in line with the results for the dimers. On the other hand, in view of the CASSCF and CAS-PT2 couplings for the guanine−adenine and guanine−thymine stacks (Table 3), one expects that in the trimers CAS-PT2 couplings will be smaller than the CASSCF results.

The electronic couplings were estimated using the two- and three-state models. Recently, it has been shown that the two-state scheme fails to provide accurate values of donor−acceptor electronic couplings for hole transfer in DNA π-stacks because of multistate effects.[40] In Table 4, we compare the couplings estimated within the two-state and multistate schemes. In the GAG stack, the couplings between neighboring bases V_{db} (G−A) and V_{ba} (A−G) do not change essentially when the bridge state is accounted for. According to the CASSCF calculation, V_{db} values found within the three- and two-state models are 0.036 and 0.049 eV, respectively, while the matrix element V_{ba} does not practically change. Similar results are obtained also with KTA. As expected, the couplings between neighboring bases agree well with the corresponding data calculated for dimers GA and AG (0.054 and 0.045 eV, Table 3). However, the donor−acceptor coupling depends considerably on the number of states treated simultaneously within the GMH scheme. In GAG, the CASSCF V_{da} values (electronic couplings between guanines) estimated within the three- and two-state models are 0.021 and 0.013 eV, respectively; the values differ by a factor of 1.6. Also, within KTA, we obtain that the three-state V_{da} coupling is by a factor of 1.5 stronger than the two-state value. Qualitatively similar results are found for the GTG stack.

It is worth noting that the donor−acceptor electronic coupling V'_{da} calculated within the two-state model can be considerably improved by taking into account the superexchange correction[38]

$$\tilde{V}_{da} = V'_{da} + V'_{db} V'_{ba}/\Delta \qquad (6)$$

where Δ can be estimated as $\Delta = \Delta E_{13} - \Delta E_{12}/2$ and the couplings V'_{da}, V'_{db}, and V'_{ba} are calculated within the two-state model applied to the whole donor−bridge−acceptor system (d−b−a) rather than to its fragments d−a, d−b, and b−a as commonly used in the superexchange model (see below). Employing, for instance, the CASSCF matrix elements presented in Table 4, we find that the $\tilde{V}_{da}$ values for GAG and GTG are equal to 0.022 and 0.007 eV, respectively, which are very close to the CASSCF couplings estimated with the three-state model.

The comparison of the CASSCF and KTA results for trimers (Table 4) with the data obtained for the dimers (Table 3) shows similar trends for the two methods. The couplings G_1T_2 and G_1A_2 in the trimers are significantly smaller than in the isolated pairs. For example, the couplings calculated with equivalent active spaces (4 orbitals per base) are 0.078 eV for the G_1T_2 pair of GTG (Table 4) and 0.098 eV in isolated GT (Table 3). A similar trend is observed for the G_1A_2 coupling. Then, the couplings between the bridge and G_3 are similar to the V values obtained for the corresponding dimers, for example, 0.087 eV for T_2G_3 in GTG (Table 4) and 84.5 meV for isolated TG (Table 3), at the CASSCF level.

Interestingly, the V_{da} value in GTG is remarkably smaller than in GAG while both V_{db} and V_{ba} are stronger. This is due

to the difference in the tunneling energy gaps. The energy of the bridge state in GTG lies remarkably higher than in GAG (the CASSCF excitation energies are 1.24 and 0.34 eV, respectively). The effects of the tunneling gap on the donor−acceptor coupling were considered in detail by Tong et al.[13] and Beljonne et al.[41]

Finally, we consider the role of the bridge in mediating the coupling. To estimate the through-space guanine−guanine interaction in the trimers GAG and GTG, we carried out calculations of a model system G_G, which was generated by removing the adenine base from GAG. The computational results are presented in Table 3. The through-space interaction of guanines in G_G is by 2−3 orders of magnitude weaker than the bridge-mediated coupling in GAG and GTG, and therefore, the intervening nucleobase completely determines the efficiency of the hole transfer between guanines in GAG and GTG.

In systems where the donor and acceptor are separated by a bridge, V_{da} may be also estimated using the superexchange approach.[26] For GBG (B = A or T), we have

$$V_{da}^{SE} = V_{G\_G} + V_{G-B}V_{B-G}/\Delta \qquad (7)$$

where $\Delta = \Delta E_{13} - \Delta E_{12}/2$ and the couplings are taken from Table 3. The effect of the direct coupling (through-space interaction) V_{G_G} may be neglected. On the basis of the CASSCF data ($\Delta = 0.286$ and 1.150 eV for B = A and T, respectively), we obtain that V_{da}^{SE} in GAG and GTG is about 0.009 and 0.008 eV, respectively. While V_{da}^{SE} found for GTG agrees well with reference value 0.007 eV (Table 4), the V_{da}^{SE} value in GAG is two times smaller than the CASSCF coupling of 0.021 eV. Also, the superexchange couplings based on KTA data are considerably smaller than the corresponding estimates derived from the calculations of GAG and GTG. In particular, for GAG, the $V_{da}^{SE} = 0.017$ eV which is only half as large as $V_{da} = 0.037$ eV given in Table 4. Thus, the donor−acceptor couplings calculated for DNA stacks within eq 7 appear to be of limited accuracy. The main difference between the superexchange approaches, eq 6 and eq 7, is as follows. In the first case, the "direct" donor−acceptor coupling V'_{da} is calculated for the whole d−b−a complex and usually it is of the same order of magnitude as the superexchange correction.[38] In the second case, the direct interaction between the donor and acceptor sites separated by an intervening nucleobase is essentially smaller than the superexchange correction and can be neglected.

Conclusions

(1) CASSCF and CAS-PT2 calculations have been performed for the ground and excited states of radical-cation systems consisting of two and three nucleobases. Electronic couplings for hole transfer in the π-stacks have been estimated using the GMH approach. The calculated excitation energies, transition dipole moments, electronic couplings, and excess charge distribution have been tabulated and can be used to assess the results obtained within less accurate approaches.

(2) The charge-transfer properties derived from the orbital energies and coefficients of HOMOs obtained with the Hartree−Fock scheme for the neutral closed-shell stacks (Koopmans' theorem approximation) were compared with the CASSCF and CAS-PT2 results. KTA provides a reasonable estimation of the excitation energies corresponding to hole transfer between nucleobases, with a tendency to overestimate the energy gaps. It also reproduces qualitatively the charge distribution predicted by the CASSCF method, where the charge is largely localized on a single base. Quantitatively, however, KTA underestimates the charge localization resulting in larger transition dipole moments than with CASSCF. The differences in excitation energies, and particularly in transition dipole moments, are the source of the overestimated electronic couplings derived from the KTA calculation as compared with the CASSCF/CAS-PT2 values.

(3) Comparing the donor−acceptor couplings in GAG and GTG calculated within two- and three-state GMH schemes, we found that the two-state treatment fails to provide reasonable estimates.

(4) On the basis of CASSCF results, we consider the role of thymine and adenine bridges in mediation of the donor−acceptor electronic coupling for hole transfer in the single-strand GAG and GTG stacks. Thus, the through-space G−G coupling is negligibly weak compared with the bridge-mediated coupling obtained with the GMH three-state scheme. In addition to that, because of partial charge localization on the adenine bridge, the superexchange approach based on the donor−bridge and bridge−acceptor couplings calculated for isolated nucleobase pairs does not give accurate estimates for the donor−acceptor couplings of GAG.

It is worth noting that the couplings in DNA stacks strongly depend on the position of nucleobases and therefore are very sensitive to conformational changes (thermal fluctuations) of the system.[42,43] The time scale of these fluctuations can be comparable with that for charge transfer. A possible approach to estimate the donor−acceptor couplings along the molecular dynamic trajectory may be based on a semiempirical expression (similar to the one suggested by Troisi and Orlandi[43]), parametrized using CASSCF results for small stacks.

Acknowledgment. This work has been supported by the Spanish Ministerio de Educación y Ciencia, Project No. CTQ2005-04563, by a grant from the Francesca Roviralta Foundation, and by a research grant from the Universitat de Girona (Ref. 7E200402).

Supporting Information Available: Complete refs 29 and 30, Mulliken charges on radical cations of isolated bases (Tables SI1a−SI1c), CASSCF and CAS-PT2 absolute energies of ground and excited states (Table SI2), dipole moment differences and transition dipole moments for the dimers and trimers (Table SI3), and Cartesian coordinates for dimer and trimer stacks. This material is available free of charge via the Internet at http://pubs.acs.org.

References and Notes

(1) Shuster, G. B, Ed. Long-Range Charge Transfer in DNA. In *Topics in Current Chemistry*; Springer: Berlin, Germany, 2004; Vol. 236, p 237.
(2) Schuster, G. B. *Acc. Chem. Res*. **2000**, *33*, 253.
(3) Giese, B. *Acc. Chem. Res*. **2000**, *33*, 631.
(4) Lewis, F. D.; Letsinger, R. L.; Wasielewski, M. R. *Acc. Chem. Res.* **2001**, *34*, 159.
(5) O'Neill, M. A.; Barton, J. K. *Top. Curr. Chem.* **2004**, *236*, 67.
(6) Endres, R. G.; Cox, D. L.; Singh, R. R. P. *Rev. Mod. Phys.* **2004**, *76*, 195.
(7) Bixon, M.; Giese, B.; Wessely, S.; Langenbacher T.; Michel-Beyerle, M. E.; Jortner, J. J. *Proc. Natl. Acad. Sci. U.S.A.* **1999**, *96*, 11713.
(8) Bixon, M.; Jortner, J. *J. Am. Chem. Soc.* **2001**, *123*, 12556.
(9) Bixon, M.; Jortner, J. *Chem. Phys.* **2002**, *281*, 393.
(10) Berlin, Y. A.; Burin, A. L.; Ratner, M. A. *J. Phys. Chem. A* **2000**, *104*, 443.
(11) Berlin, Y. A.; Burin, A. L.; Ratner, M. A. *J. Am. Chem. Soc*. **2001**, *123*, 260.
(12) Berlin, Y. A.; Burin, A. L.; Ratner, M. A. *Chem. Phys.* **2002**, *275*, 61.
(13) Tong, G. S. M.; Kurnikov, I. V.; Beratan, D. N. *J. Phys. Chem. B* **2002,** *106*, 2381.

(14) Voityuk, A. A.; Rösch, N.; Bixon, M.; Jortner, J. *J. Phys. Chem. B* **2000**, *104*, 9740.
(15) Voityuk, A. A.; Bixon, M.; Jortner, J.; Rösch, N. *J. Chem. Phys.* **2001**, *114*, 5614.
(16) Jortner, J.; Bixon, M.; Voityuk, A. A.; Rösch, N. *J. Phys. Chem. A* **2002**, *106*, 7599.
(17) Berlin, Y. A.; Kurnikov, I. V.; Beratan, D. N.; Ratner, M. A.; Burin, A. L. *Top. Curr. Chem.* **2004**, *237*, 1−36.
(18) Senthilkumar, K.; Grozema, F. C.; Guerra, C. F.; Bickelhaupt, F. M.; Lewis, F. D.; Berlin, Y. A.; Ratner, M. A.; Siebbeles, L. D. A. *J. Am. Chem. Soc.* **2005**, *127*, 14894.
(19) Giese, B. *Nature* **2001**, *412*, 318.
(20) Giese, B.; Spichty, M. *Chem. Phys. Chem.* **2000**, *1*, 195.
(21) Conwell, E. M. *Proc. Natl. Acad. Sci. U.S.A.* **2005,** *102*, 8795.
(22) Liu, C.-S.; Hernandez, R.; Schuster, G. B. *J. Am. Chem. Soc.* **2004**, *126*, 2877.
(23) Voityuk, A. A. *J. Chem. Phys.* **2005**, *122*, 204904.
(24) Basko, D. M.; Conwell, E. M. *Phys. Rev. Lett.* **2002**, *88*, 098102.
(25) Marcus, R. A.; Sutin, N. *Biochim. Biophys. Acta* **1985**, *811*, 265.
(26) Newton, M. D. *Chem. Rev.* **1991**, *91*, 767.
(27) Rösch, N.; Voityuk, A. A. *Top. Curr. Chem.* **2004,** *237*, 37−72.
(28) Dreuw, A.; Head-Gordon, M. *Chem. Rev.* **2005,** *105*, 4009.
(29) Frisch, M. J.; et al. *Gaussian 03*; Gaussian, Inc.: Pittsburgh, PA, 2003.
(30) Andersson, K.; et al. *MOLCAS*, version 5.4; University of Lund: Lund, Sweden, 2003.
(31) Cave, R. J.; Newton, M. D. *J. Chem. Phys.* **1997**, *106*, 9213.
(32) Cave, R. J.; Newton, M. D. *Chem. Phys. Lett.* **1996**, *249*, 15.
(33) Clowney, L.; Jain, S. C.; Srinivasan, A. R.; Westbrook, J.; Olson, W. K.; Berman, H. W. *J. Am. Chem. Soc.* **1996**, *118*, 509.
(34) Lu, X. J.; El Hassan, M. A.; Hunter, C. A. *J. Mol. Biol.* **1997**, *273*, 681.
(35) Yoshioka, Y.; Kitagawa, Y.; Tukano, Y.; Yamaguchi, K.; Nakamura, T.; Saito, I. *J. Am. Chem. Soc.* **1999**, *121*, 8712.
(36) Voityuk, A. A.; Jortner, J.; Bixon, M.; Rösch, N. *Chem. Phys. Lett.* **2000**, *324*, 430.
(37) Voityuk, A. A. *J. Phys. Chem. B* **2005**, *109*, 10793.
(38) Voityuk, A. A. *J. Chem. Phys.* **2006**, *124*, 064505.
(39) Voityuk, A. A.; Jortner, J.; Bixon, M.; Rösch, N. *Chem. Phys. Lett.* **2000**, *324*, 430.
(40) Voityuk, A. A. *J. Phys. Chem. B* **2005**, *109*, 17917.
(41) Beljonne, D.; Pourtois, G.; Ratner, M. A.; Bredas, J. L. *J. Am. Chem. Soc.* **2003**, *125*, 14510.
(42) Voityuk, A. A.; Siriwong, K.; Rösch, N. *Phys. Chem. Chem. Phys.* **2001**, *3*, 5421.
(43) Troisi, A.; Orlandi, G. *J. Phys. Chem. B* **2002**, *106*, 2093.